Korean Journal of Microbiology (2018) Vol. 54, No. 4, pp. 343-353
DOI https://doi.org/10.7845/kjm.2018.8051

pISSN 0440-2413
eISSN 2383-9902

Integrative analysis of cellular responses of *Pseudomonas* sp. HK-6 to explosive RDX using its *xenA* knockout mutant

Bheong-Uk Lee[1], Moon-Seop Choi[2], Ji-Won Seok[2], and Kye-Heon Oh[2*]

[1]*Division of Biological Sciences and Chemistry, Kosin University, Busan 49104, Republic of Korea*
[2]*Department of Life Science and Biotechnology, Soonchunhyang University, Asan 31091, Republic of Korea*

Pseudomonas sp. HK-6의 *xenA* 돌연변이체를 이용하여 RDX 폭약에 노출된 세포반응들의 통합적 분석

이병욱[1] · 최문섭[2] · 석지원[2] · 오계헌[2*]

[1]고신대학교 의생명과학과, [2]순천향대학교 생명시스템학과

(Received July 25, 2018; Revised September 10, 2018; Accepted September 10, 2018)

Our previous research demonstrated the essential role of the *xenB* gene in stress response to RDX by using *Pseudomonas* sp. HK-6 *xenB* knockout. We have extended this work to examine the cellular responses and altered proteomic profiles of the HK-6 *xenA* knockout mutant under RDX stress. The *xenA* mutant degraded RDX about 2-fold more slowly and its growth and survival rates were several-fold lower than the wild-type HK-6 strain. SEM revealed more severe morphological damages on the surface of the *xenA* mutant cells under RDX stress. The wild-type cells expressed proportionally-increased two stress shock proteins, DnaK and GroEL from the initial incubation time point or the relatively low RDX concentrations, but slightly less expressed at prolonged incubation period or higher RDX. However the *xenA* mutant did not produced DnaK and GroEL as RDX concentrations were gradually increased. The wild-type cells well maintained transcription levels of *dnaA* and *groEL* under increased RDX stress while those in the *xenA* mutant were decreased and eventually disappeared. The altered proteome profiles of *xenA* mutant cells under RDX stress also observed so that the 27 down-regulated plus the 3 up-regulated expression proteins were detected in 2-DE PAGE. These all results indicated that the intact *xenA* gene is necessary for maintaining cell integrity under the xenobiotic stress as well as performing an efficient RDX degradation process.

Keywords: *Pseudomonas* sp. HK-6, *xenA* gene, proteomic analysis, RDX stress

***For correspondence.** E-mail: kyeheon@sch.ac.kr;
Tel.: +82-41-530-1353; Fax: +82-41-530-1493

Hexahydro-1,3,5-trinitro-1,3,5-triazine (RDX) is one of the most powerful and commonly used military explosives and is released into ecosystems principally as the result of military activities (Juhasz and Naidu, 2007). RDX is s toxic compound that threatens public health as a consequence of this contamination, and has been proposed as a possible human carcinogen (McLellan *et al*., 1992). The widespread contamination by RDX necessitates the remediation processes of contaminated soil and groundwater. Studies have reported on the biodegradation of RDX in water and soil (Kitts *et al*., 1994; Ronen *et al*., 2008). Many bacterial and fungal isolates, including *Pseudomonas* sp., *Stenotrophomonas* sp., and *Rhodococcus* sp., are known to be capable of metabolizing RDX, and many different types of intermediates and end products have been identified (Binks *et al*., 1995; Fuller *et al*., 2010; Lee *et al*., 2013).

Extensive researches on the biodegradation of RDX have been performed over the last decades. Most of the researches

were carried out anaerobically on environmental samples such as soil, sewage sludge, horse manure compost, and so on (Osman and Klausmeiser, 1973; McCormick *et al*., 1981; Kitts *et al*., 1994). Relatively small numbers of aerobic RDX degradation have been reported (Binks *et al*., 1995). Although most researches have focused on the ecological and metabolic aspects of the RDX-degrading isolates, several enzymes (especially xenobiotic nitroreductase) that are involved in RDX biodegradation have been the target of considerable interest for the development of cost-effective biological alternatives, such as the construction of transgenic microorganisms or plants (Jackson *et al*., 2007; Fuller *et al.*, 2009; Lorenz *et al.*, 2012).

The degradation of RDX (Fuller *et al*., 2009) and TNT (Pak *et al*., 2000) by xenobiotic reductase (XenA or XenB) from the *Ps. putida* II-B and *Ps. fluorescens* I-C has been explored in detail. Both XenA and XenB belong to the Old Yellow Enzyme (OYE) family of flavoprotein oxidoreductases, which have been found in bacteria, yeast, and plants (Williams and Bruce, 2002). These enzymes were known to more quickly transform RDX or other energetic compounds under anaerobic conditions compared to aerobic conditions (Fuller *et al*., 2009). However, very little data is available on the characteristics of the involvement of xenobiotic reductase A (XenA) in the biodegradation of RDX. We previously reported the characterization of the *xenB* mutant under RDX stress (Lee *et al*., 2015). In many aspects, the results obtained from the *xenA* mutant were quite similar to those of the *xenB* mutant, yet it would be worthy of comparing of them.

In order to investigate the role of *xenA* gene in RDX degradation process and under RDX stress condition, the *Pseudomonas* sp. HK-6 *xenA* mutant was constructed by a homologous recombination with a partial *xenA* gene fragment lacking start and stop codons. Several aspects of the *xenA* mutant were compared with the wild-type strain in order to elucidate the role of this gene in RDX biodegradation and the stress response. The RDX degradability by the *xenA* mutant was measured and compared to the wild-type bacteria under aerobic conditions. The survival rates and the expression levels of the stress shock proteins (SSPs) DnaK and GroEL under RDX stress were examined. In addition, mRNA expression levels of *xenA* mutant and wild-type cells were examined under RDX stress. Furthermore, scanning electron microscopy (SEM) analysis was carried out to see the morphological changes occurred in the cell envelope of both strains after RDX exposure. Finally, the different proteome profiles of the wild-type HK-6 strain and the *xenA* mutant under RDX stress were compared.

Materials and Methods

Bacterial strains, culture conditions and molecular manipulation of the *xenA* gene

For RDX degradation, HK-6 cells were grown in liquid medium composed of 25–75 μM RDX, 10 mM K_2HPO_4, 5 mM NaH_2PO_4, 1 mM $MgSO_4 \cdot 7H_2O$, 0.07 mM $CaCl_2 \cdot 2H_2O$, 0.04 mM $FeCl_3 \cdot 6H_2O$, 0.0005 mM $MnCl_2 \cdot 4H_2O$, and 0.00035 mM $ZnSO_4 \cdot 7H_2O$ and 2 mM fructose as a supplemental carbon source. The aerobic cultivation and maintenance of *Pseudomonas* strains have been previously described in detail (Chang *et al*., 2004).

The *xenA* knockout mutant was constructed by integration of a 931-bp internal DNA fragment into the HK-6 *xenA* original locus. An internal DNA fragment of *xenA* was amplified with the primers 5'-AATTCAAGCTTGCTGCCGTGCCGACGAAG-3' and 5'-AATTGAATTCTCGTTCAGTGGCGCATCC-3'. The partial *xenA* DNA product was inserted in pBGS18 and transformed into HK-6 cells, and its integration in the original *xenA* locus was confirmed by another PCR with chromosomal DNA as a template. Other molecular manipulation techniques were performed as described by Miller (1972).

Survival test

The wild-type and *xenA* mutant cells grown on Luria-Bertani (LB) media were harvested by centrifugation at 2,000 × *g* for 10 min. These cells were washed three times with 10 mM phosphate buffer (pH 7.0), and then inoculated to approximately 10^7 cells/ml of liquid basal medium in 100 ml Erlenmeyer flasks containing 25, 50, or 75 μM RDX. The cell survival was examined by removing aliquots of cells at selected intervals during 60 days of incubation; then, the colonies were counted by plating them on LB agar incubated at 30°C.

SDS–PAGE, western blot, and real–time qPCR analyses

RDX-treated cells were analyzed to analyze for the expression

of the SSPs, DnaK, and GroEL by Western blot technique with anti-DnaK and anti-GroEL monoclonal antibodies (StressGen Biotechnologies Corp.), which were induced by heat shocking *Escherichia coli* (70 kDa for DnaK and 60 kDa for GroEL). Isolation of the SSPs from the HK-6 wild-type and *xenA* mutant strains was performed using 12% acrylamide for the separating gel and 5% acrylamide for the stacking gel according to the methods described by Bollag *et al.* (1996). Western blot analysis was performed by methods with some modification, described by Lee *et al.* (2000).

Total RNA was extracted from the wild-type and *xenA* mutant cells with an RNA extraction kit (Macherey-Nagel Inc.) according to the manufacturer's instructions. Then, total RNA was treated with RNase-free DNase and quantified at 260 nm with a Tecan Multi-Reader spectrometer (Männodorf). For RT-qPCR analysis, we used *dnaK-F/dnaK-R*, *groEL-F/groEL-R* and internal control primers 16S rRNA-F/16S rRNA-R (Table 1). RT-qPCR analysis was performed using an iScript™ One-Step RT-qPCR kit with SYBR Green (Bio-Rad) in a Bio-Rad CFX96 RT-PCR System. RT-qPCR samples were run in triplicate, and the data were analyzed using the Bio-Rad CFX Manager software.

SEM analysis

Colonies of wild-type HK-6 and the *xenA* mutant grown on LB agar plates for 24 h were excised as small agar blocks. The agar blocks that containing a colony were then exposed to 50 μM RDX in minimal salt medium for 8 h. Both wild-type and *xenA* mutant cells were fixed, dehydrated, air dried, and coated with gold and examined under a Hitachi S-2500C scanning electron microscope (SEM) (Hitachi) as previously described (Ng *et al*., 1985).

Proteomic analysis

Two-dimensional electrophoresis (2-DE) was performed with the proteomes from the wild-type and *xenA* mutant cells treated with 50 μM RDX. A 2-DE analysis was conducted according to previously described methods (Heukeshoven and Dernick, 1985; Kim *et al*., 2002). The protein spots were excised from the silver-stained 2-D gels and digested with trypsin in accordance with the previously described technique (Ho *et al*., 2004). The MALDI fingerprint data were analyzed using MS-Fit (http://prospector.ucsf.edu/prospector/4.0.8/html/msfit.htm) against the NCBI database (Perkins *et al.*, 1999).

Results and Discussion

Construction of the *xenA* knockout mutant

The complete 1,092 bp *xenA* gene was amplified from the HK-6 strain using PCR primers 5'-ATGGATCCACCACGCT TTTCGATCCGATC-3' and 5'-ATCCCTGCAGTCACAACC GCGGATAATCGATG-3' which were designed based on the previously reported *xenA* gene sequences in GenBank. The deduced amino acid sequences of XenA from HK-6 showed 99% and 94% identity to those from *Ps. putida* KT2440 and *Ps. fluorescens*, respectively (data not shown). The preliminary crystal structure of XenA from *Ps. fluorescens* I-C was determined to a 2.3 Å resolution (Orville *et al*., 2004) and the substrate-binding amino acid residues of XenA have been determined (Spiegelhauer *et al*., 2010). A multiple sequence alignment of 40 previously reported OYEs revealed two conserved active sites (HG and YGGS) (Nizam *et al*., 2014), which were also present in the HK-6 XenA protein (data not shown). However, the amino acid residues that are essential for the catalytic reactions of XenA require further elucidation.

Table 1. PCR primers used in this study

Primer	Sequence	Source or reference
dnaK-F	5'-TTCGGTCATCGAAATCGCCGAAGT-3'	This work
dnaK-R	5'-TGCCCGACTCTTTCTTGAACTCGT-3'	This work
groEL-F	5'-ATCCGTGCCCAGATCG1AAGAAACT-3'	This work
groEL-R	5'-CAACGCGGGCTTTCTTCTCTTTCA-3'	This work
16S rRNA-F	5'-AAGGAACACCAGTGGCGAAGG-3'	This work
16S rRNA-R	5'-CCAGGCGGTCAACTTAATGCG-3'	This work

To construct the *xenA* null mutant, a 931 bp-long internal *xenA* gene fragment lacking both initiation and termination codons was amplified and inserted into pBGS18 and transformed into the HK-6 strain. The transformed internal *xenA* fragment was integrated into its original locus via single crossover homologous recombination. This event resulted in the generation of two nonfunctional partial *xenA* genes: one that did not have the start codon and another that did not have the stop codon. The integration of the partial *xenA* fragment also conferred kanamycin-resistance, which was attributed by the presence of the simultaneously integrated pBGS18 plasmid. To verify the proper integration of the plasmid harboring the partial *xenA* DNA fragment, the entire chromosome of the putative *xenA* mutant was purified and subjected to PCR with primers that targeted a portion of the plasmid DNA sequence. In the *xenA* mutant, the amplified DNA fragment from the inserted plasmid was detected; however, it was not detected in the wild-type strain (data not shown).

Comparative degradation of RDX between HK-6 wild-type and its *xenA* mutant

A previous study reported that XenA of *Ps. Fluorescens* I-C was able to transform RDX under aerobic and anaerobic conditions, although the degradation rate was always faster under anaerobic conditions (Fuller *et al*., 2009). To examine the role of *xenA* in a RDX degradation process, the residual RDX in the supernatants of aerobic cultures of the HK-6 and the *xenA* mutant cells was measured (Fig. 1). HK-6 was shown to completely degrade 25 and 50 μM RDX in 40 and 50 days, respectively (Fig. 1A and B). However, the *xenA* mutant degraded less than 30% of the RDX over the same time period. Even after 60 days of aerobic incubation, the *xenA* mutant achieved only approximately 27% and 21% degradation of 25 and 50 μM RDX, respectively. About 52% of the RDX was still remained in the supernatant of HK-6 aerobic culture which contained 75 μM RDX (Fig. 1C). Taken altogether, XenA appeared to be an important enzyme in the RDX degradation pathways, yet it was not the only enzyme involved in the process since the *xenA* knockout mutant also more or less showed an ability to reduce The concentration of RDX. This means that there are at least more than two degradation pathways of RDX exist in the HK-6 strain. No metabolic intermediates during RDX degradation were detected by HPLC in this work.

Survival rates and scanning electron microscopy

The survival rates of the *xenA* mutant were 10^2–10^4-fold lower than the rates of the HK-6 strain in the presence of 25, 50, and 75 μM RDX (Fig. 2A and B). It may need a further investigation to find precise reasons of this higher lethality of *xenA* mutant. However it may be partly caused by a higher concentration of RDX in the media due to the slower degrada-

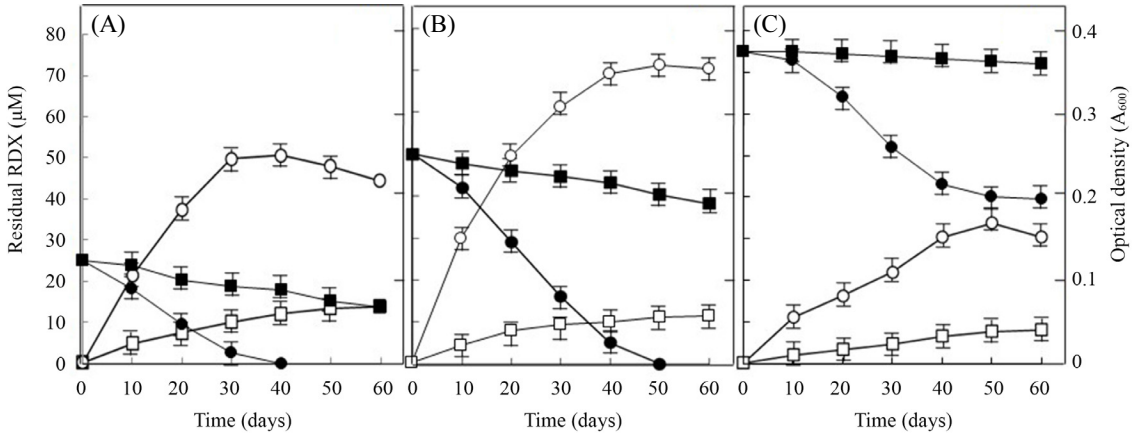

Fig. 1. Bacterial growth (open symbol) and RDX degradation (closed symbol) of wild-type (circle) and the *xenA* knockout mutant (square) of *Pseudomonas* sp. HK-6. The growth rate was measured as the optical density at 600 nm, and the rate of RDX degradation was determined by HPLC every 10 days throughout the 60-day incubation period. In this experiment, RDX was initially supplied at concentrations of 25 (A), 50 (B), and 75 μM (C), respectively. The error bars indicate the standard deviations of the means.

tion rate of the *xenA* mutant.

Several studies reported that aromatic hydrocarbons at high concentrations induced toxic effects on the cells due to the disruption of membrane components (Ramos *et al*., 1995; Sikkema *et al*., 1995), ultimately leading to cell death. We also previously showed that toxic chemicals have substantial cytotoxic impacts on target cells, causing perforations and changes in shape; these changes can be observed under scanning electron microscopy (Chang *et al*., 2004; Lee *et al*., 2008a). To observe morphological cellular changes after exposure to RDX, the wild-type and *xenA* mutant cells were cultured in LB broth supplemented with 50 μM RDX for 8 h. Both wild-type cells and *xenA* mutant cells grown in LB medium without RDX exhibited a typical rod shape with a smooth surface (data not shown). Obvious morphological change was little observed in wild-type cells treated with 50 μM RDX for 8 h (Fig. 3A). However significant morphological changes were shown in the *xenA* mutant cells under the same conditions (Fig. 3B). The *xenA* mutant had several destructive openings and a higher frequency of irregular rod forms with wrinkled cell surfaces. These results indicated that the removal of toxic RDX by XenA might not be a sole reason to keep cell integrity; nonetheless, it probably did help it. In addition to this, two stress shock proteins (SSPs), DanK and GroEL appeared not to be sufficiently expressed

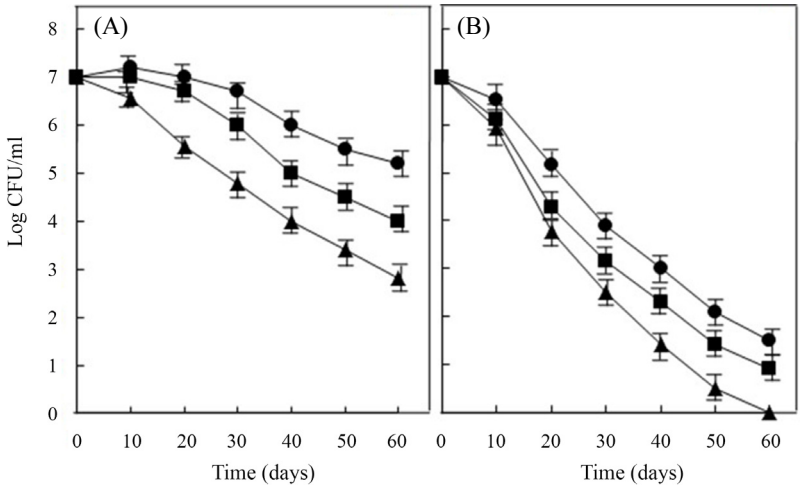

Fig. 2. Survival rates of wild-type (A) and *xenA* mutant (B) *Pseudomonas* sp. HK-6 following exposure to RDX. The cells were exposed to concentrations of 25 (circle), 50 (square), and 75 μM (triangle) RDX. At intervals, the number of colonies (CFU/ml) was measured. The error bars indicate the standard deviations of the means.

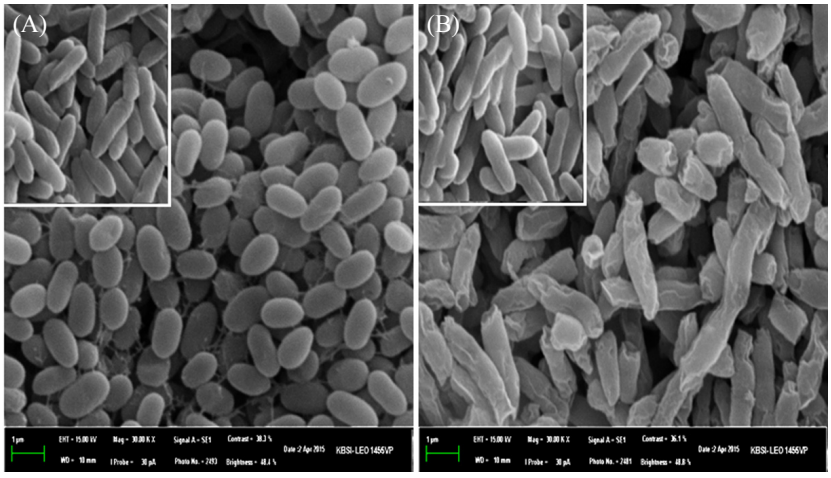

Fig. 3. Scanning electron micrographs of the wild-type (A) and its *xenA* mutant (B) of *Pseudomonas* sp. HK-6 treated with 50 μM RDX for 8 h. The upper left in each micrograph includes the control strains.

Table 2. Comparative analysis of RDX-induced proteins in *Pseudomonas* sp. HK-6 and its *xenA* mutant strain by MALDI-TOF fingerprinting

Spot No.	Identification protein	GenBank ID	Sequence coverage (%)	Fold change WT/MT
Chaperones				
1	DnaK	YP_004703984	54	↑/-
2	GroEL	WP_016713585	21	↑/-
3	Trigger factor	YP_008762569	36	↑/-
Metabolism				
4	Xenobiotic reductase A, XenA	NP_743414	57	↑/-
5	NAD(P)H quinone oxidoreductase	WP_004575816	33	↑/-
6	Membrane dipeptidase	YP_001666580	28	↑/-
7	Ribose-phosphate pyrophosphokinase, PRPS1	YP_001266104	40	↑/-
8	Bifunctional aconitate hydratase 2/2-methyl isocitrate dehydratase, AcnB	YP_001268741	34	↑/-
9	2,3,4,5-Tetrahydropyridine-2,6-carboxylate N-succinyltransferase	NP_743687	33	↑/-
10	NAD synthetase	WP_019098913	36	↑/-
11	Gamma-carboxygeranoyl-CoA hydratase, LiuC	WP_019096338	38	↑/-
12	Aldo-keto reductase	WP_019098042	25	↑/-
13	2-Oxoisovalerate dehydrogenase subunit beta, BCKDHB	YP_008092422	60	-/↑
Transcription, Translation, and Biosynthesis				
14	Elongation factor G, EF-G	WP_019096593	38	↑/-
15	Polynucleotide phosphorylase/polyadenylase, Pnp	WP_023048994	24	↑/-
16	Adenylosuccinate synthetase	WP_019097351	42	↑/-
17	Cysteine desulfurase	NP_743003	29	↑/-
18	DNA-directed RNA polymerase subunit alpha, rpoA	YP_008111549	42	↑/-
19	Elongation factor P, EF-P	WP_009406582	53	↑/-
20	Putative dihydroorotate	YP_008116103	36	↑/-
Transport, Binding protein, and Protein export				
21	Ribosome-binding factor A, RbfA	YP_004703968	67	↑/-
22	Glycine/betaine ABC transporter substrate-binding protein	WP_019096855	22	↑/-
23	Branched-chain amino acid ABC transporter substrate-binding protein	YP_008097608	30	↑/-
24	Amino acid ABC transporter, periplasmic binding protein, AapJ	YP_005932045	53	↑/-
25	Extracellular solute-binding protein	YP_001747778	60	↑/-
26	Iron ABC transporter substrate-binding protein	WP_019098100	52	↑/-
Secondary metabolites biosynthesis				
27	Phenylacetate-CoA oxygenase subunit, PaaI	NP_745419	32	↑/-
Cell envelope				
28	Outer membrane protein, OprQ	AAN65899	28	↑/-
29	Outer membrane protein H1, OprH	YP_004703451	56	-/↑
Signal transduction				
30	Alginate biosynthesis sensor histidine kinase/GAF domain protein	AAN70807	35	-/↑

↑, Arrows indicate up-regulation of protein expression level based on comparison of protein sizes
-, not significantly changed

in *xenA* mutant background (Table 2). This probably contributed a lower survival rate as well as more damages on cell surface of *xenA* mutant.

Western blot and RE-qPCR analyses

Environmental stresses including explosives such as RDX, induce SSPs. The expression levels of the 70-kDa DnaK and

60-kDa GroEL proteins under RDX stress conditions in the HK-6 wild-type and the *xenA* mutant were compared using SDS-PAGE and western blotting with anti-DnaK and anti-GroEL monoclonal antibodies (Fig. 4). In the wild-type, the two SSPs were induced by RDX and were found to increase in proportion to the length and concentration of the RDX treatment, which is consistent with previous observations (Fig. 4A, B, and C) (Chang *et al.*, 2004). However, the fates of the two SSPs in the *xenA* mutant appeared to be quite different. Both DnaK and GroEL were more highly expressed in the *xenA* mutant in the absence of RDX (Fig. 4D, E, and F). However, the levels of the two SSPs began to decrease in proportion to the elapsed treatment time in the presence of 50 μM RDX. Interestingly, DnaK and GroEL exhibited a small amount of expression in the presence of 50 and 75 μM RDX, while their expression appeared to be enhanced in the presence of 25 μM RDX. The levels of relative gene expression measured by RT-qPCR were consistent with the western blotting results (Fig. 5). The expression of the *dnaK* and *groEL* genes was reduced in the XenA genetic background. These results indicated that increased lethality and other phenotypic changes might occur in the presence of RDX stress due to the limited expression of these SSPs. Many SSPs, such as DnaK and GroEL, are chaperone proteins that assist in the proper folding of essential enzymes under environmental stress conditions.

Analysis of the proteome profiles

The proteomic profiles of the wild-type and *xenA* mutant cells cultured in LB medium in the presence of RDX were compared (Fig. 6). A total of 30 unambiguous spots were extracted, digested with trypsin, and analyzed by MALDI-TOF MS. The MALDI-TOF MS analysis was independently conducted

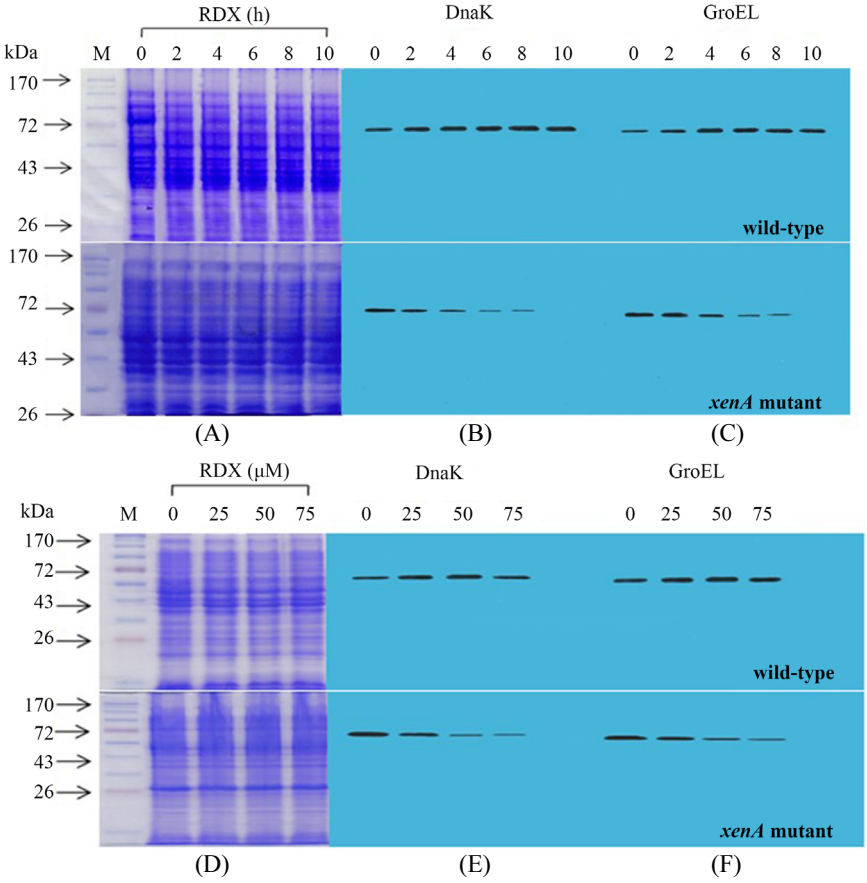

Fig. 4. Induction of stress shock proteins (SSPs) in wild-type and *xenA* mutant *Pseudomonas* sp. HK-6 treated with 50 μM RDX for different exposure times (A, B, and C), and for different RDX concentrations (D, E, and F). The SSPs were analyzed by SDS-PAGE (A, D) and western blot with anti-DnaK (B, E) and anti-GroEL (C, F) monoclonal antibodies. The initial colony-forming units per ml (CFU/ml) were approximately 1.46×10^8, and samples with equal amounts of protein (40 μg) were subjected to western blotting.

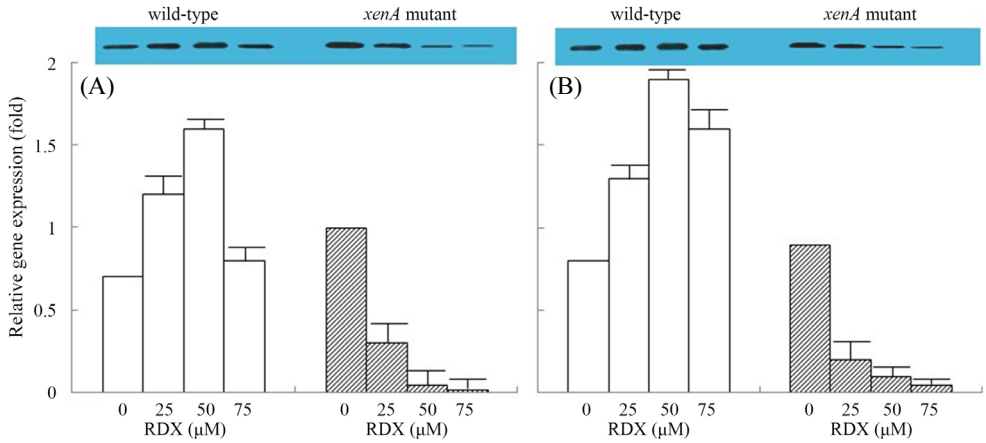

Fig. 5. Analysis of *dnaK* (A) and *groEL* (B) gene expression under RDX stress conditions. Induction of the *dnaK* and *groEL* genes in cells treated with 0, 25, 50, and 75 μM RDX for 8 h. The DnaK and GroEL concentrations were analyzed using western blotting with the anti-DnaK and anti-GroEL monoclonal antibodies, and *dnaK* and *groEL* gene expression was measured using RT-qPCR of the wild-type (square) and *xenA* (shaded square) mutant cells. The numbers on the x-axis of the RT-qPCR graph and above the western blot photos indicate the time points for the samples collected. The numbers on the y-axis represent relative gene expression.

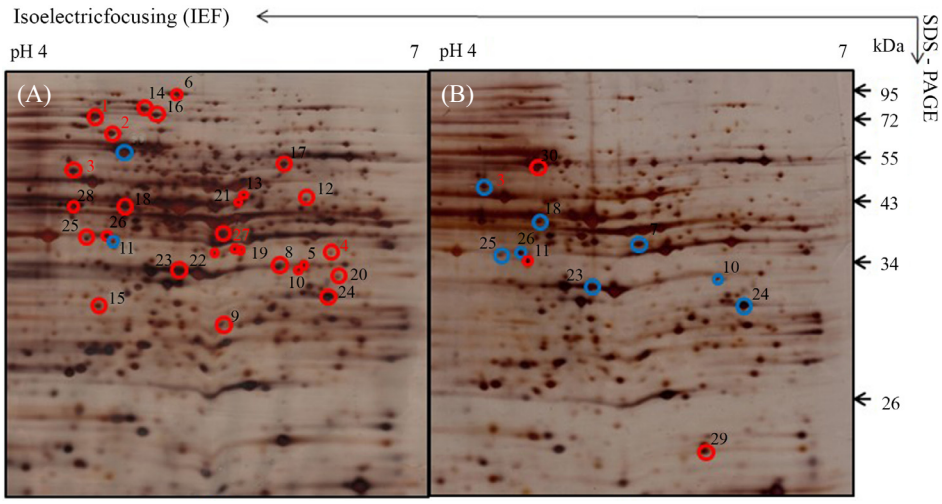

Fig. 6. 2-DE patterns of total proteins in wild-type (A) and *xenA* mutant (B) of *Pseudomonas* sp. HK-6. Numbers associated with the spots identified by MALDI-TOF are listed in Table 2.

at least three times. The total proteins were classified into 7 groups based on function: chaperone, metabolism, transcription and translation, transport and binding protein, secondary metabolite biosynthesis, cell envelope, and signal transduction. The MS analysis showed 27 proteins with decreased expression or no expression in the *xenA* mutant (Table 2). Interestingly, there was little or no expression of the SSPs (*e.g.*, DnaK, GroEL, and the trigger factor) in the *xenA* mutant under RDX stress despite the fact that SSPs are usually induced by stress. In fact, TNT stress was reported to cause the accumulation of the chaperones GroEL and RpoH; also these proteins were more highly accumulated in the *algA* mutant, which did not produce alginate, a matrix to potentially protect cells exposed to stresses (Lee *et al*., 2008b). Furthermore, the gene AAN70807, which is related to alginate biosynthesis, was highly induced under RDX stress conditions (Table 2). It remains unclear whether the increased expression of this gene was directly connected to the production of alginate. However, the *xenA* mutant cells would produce more alginate if they needed stronger protection against the higher concentrations of RDX.

Outer membrane (OM) proteins are involved in many aspects of growth and development of the bacterial cell (Hancock and Brinkman, 2002). In particular, OM proteins of *Ps. aeruginosa* play a significant role in membrane permeability, nutrient uptake, antibiotic resistance, and virulence at the infection site (Arhin and Boucher, 2010). Our MS analysis identified 2 OM proteins: up-regulated OprH and down-regulated OprQ. In our proteome analysis, OprH, which might be necessary for cell survival in harsh environments such as RDX exposure, was highly expressed in the *xenA* mutant. OprH has been reported to stabilize the OM by increasing its protection from membrane perturbation (Edrington *et al*., 2011). In contrast, OprQ was down-regulated and not detected in the *xenA* mutant. OprQ has been reported to participate in nutrient uptake from the environment and is involved (directly or indirectly) in the regulation of other proteins/porins that are important for *Ps. aeruginosa* growth. OprQ is also required for survival under conditions where *Ps. aeruginosa* is exposed to adverse growth conditions (Arhin and Boucher, 2010). Based on previous reports, these results indicate that the *xenA* mutant cells exposed to RDX demonstrated reduced survival due to a lack of OprQ production.

Previous comparison of proteome profiles between the wild-type and the *xenB* cells revealed 22 differently-expressed proteins (Lee *et al*., 2015). Among them, 13 proteins were consistent with those of 2-DE gels from the *xenA* mutant cells while 9 proteins were not identical in the profile of the *xenA* mutant proteome. 17 proteins from 2-DE gel in this *xenA* mutant study were newly identified. The exact roles of these differently-expressed proteins under RDX stress in *xenA* or *xenB* genetic background would not be totally understandable. However, accumulation of proteome profiles from the independently-performed analyses will generate more valuable data regarding proteins involved in xenobiotics stress responses.

The XenA protein had not been extensively studied in *Pseudomonas* species. However, there have been an increasing number of reports regarding the biodegradation or bioremediation of the RDX and TNT explosives using the XenA and XenB enzymes. A broader and more intensive understanding of the involvement of XenA in RDX biodegradation will create more opportunities for a variety of biotechnological applications. The enzyme can be improved by mutagenesis or genome shuffling techniques for a more efficient bioremediation process (Ronen *et al*., 2008). Additionally, studies of XenA, XenB, or related enzymes involved in the microbiological degradation of xenobiotics may provide information that can be used to improve the degradation function of these enzymes. Furthermore, a more powerful strain with a greater capability for RDX degradation can be developed by the introduction of the genes derived from these enzymes into a single strain, enabling the construction of transgenic microorganisms or plants that can be used for RDX bioremediation.

적 요

이전 연구에서 우리는 RDX (hexahydro-1,3,5-trinitro-1,3,5-triazine) 분해세균 *Pseudomonas* sp. HK-6에서 xenobiotic reductase B를 암호화하는 *xenB* 유전자의 돌연변이 균주를 이용하여 RDX 스트레스에 대한 *xenB* 유전자의 역할에 관하여 연구를 보고하였다[Lee *et al*. (2015) *Curr. Microbiol.* 70(1): 119–127]. 본 연구에서는 *Pseudomonas* sp. HK-6 *xenA* 돌연변이 균주로 연구 범위를 확대하여 RDX 스트레스 조건에서 세포반응과 프로테옴 프로필의 변화를 분석하였다. RDX 첨가 배지에서 *xenA* 돌연변이 균주는 야생균주와 비교하여 RDX를 약 2배 정도 느리게 분해하였으며, RDX 스트레스 하에서 *xenA* 돌연변이 균주의 생장률과 생존율은 야생균주와 비교하여 낮았다. RDX 스트레스에 의한 심한 형태적 손상이 *xenA* 돌연변이 균주의 세포 표면에 발생하는 것이 주사전자현미경을 통해서 확인되었다. RDX 스트레스 하에서 야생균주에서 발현된 충격단백질인 DnaK 및 GroEL의 양은 배양 초기 혹은 상대적으로 낮은 RDX 농도에서는 증가하였으나, 배양시간이 길어지거나 높은 RDX 농도에서는 다소 감소하였다. 그러나 *xenA* 돌연변이 균주에서는 DnaK와 GroEL의 발현양은 RDX 농도가 증가함에 따라 점차 감소되었다. RT-qPCR에 의해 측정된 야생균주에서 *dnaA*와 *groEL*의 전사 수준은 RDX 스트레스가 증가된 상태에서 잘 유지되었으나, *xenA* 돌연변이 균주에서는 점차 감소되어 결국에는 소멸되었다. RDX 스트레스에서 *xenA*의 돌연변이에 의한 프로테옴 프로필의 변화를 2-DE PAGE를 통해서 관찰한 결과에 따르면 27개 단백질이 감소하고 3개가 증가한 것으로 나타났다. 이들 결과로 보아, 정상적인 *xenA* 유전자는 RDX 스트레스 하에서 세포의 온전한 형태 유지와 효율적인 RDX 분해 과정을 수행하기 위해서 필요하다는 것을 의미하였다.

Acknowledgements

This research was supported by the Basic Science Research Program through the National Research Foundation of Korea, funded by the Ministry of Education, Science, and Technology (2011-0026690), and by the Soonchunhyang University Research Fund. We thank the ROK Agency for Defense Development for providing the RDX used in this study.

References

Arhin A and Boucher C. 2010. The outer membrane protein OprQ and adherence of *Pseudomonas aeruginosa* to human fibronectin. *Microbiology* **156**, 1415–1423.

Binks PR, Nicklin S, and Bruce NC. 1995. Degradation of hexanydro-1,3,5-trinitro-1,3,4-triazine (RDX) by *Stenotrophomonas maltophilia* PB1. *Appl. Environ. Microbiol.* **61**, 1318–1322.

Bollag DM, Rozycki MD, and Edelstein SJ. 1996. Protein methods. 2th ed. Wiley-Liss, New York, USA.

Chang HW, Kahng HY, Kim SI, Chun JW, and Oh KH. 2004. Characterization of *Pseudomonas* sp. HK-6 cells responding to explosive RDX (hexahydro-1,3,5-trinitro-1,3,5-triazine). *Appl. Microbiol. Biotechnol*. **65**, 323–329.

Edrington TC, Kintz E, Goldberg JB, and Tamm LK. 2011. Structural basis for the interaction of lipopolysaccharide with outer membrane protein H (OprH) from *Pseudomonas aeruginosa*. *J. Biol. Chem*. **286**, 39211–39223.

Fuller ME, McClay K, Hawari J, Paquet L, Malone TE, Fox BG, and Steffan RJ. 2009. Transformation of RDX and other energetic compounds by xenobiotic reductases XenA and XenB. *Appl. Microbiol. Biotechnol.* **84**, 535–544.

Fuller ME, Perreault N, and Hawari J. 2010. Microaerophilic degradation of hexahydro-1,3,5-trinitro-1,3,5-triazine (RDX) by three *Rhodococcu*s strains. *Lett. Appl. Microbiol.* **51**, 313–318.

Hancock RE and Brinkman FSL. 2002. Function of *Pseudomonas* porins in uptake and efflux. *Annu. Rev. Microbiol.* **56**, 17–38.

Heukeshoven J and Dernick R. 1985. Simplified method for silver staining of proteins in polyacrylamide gels and the mechanism of silver staining. *Electrophoresis* **6**, 103–112.

Ho EM, Chang HW, Kim SI, Kahng HY, and Oh KH. 2004. Analysis of TNT (2,4,6-trinitrotoluene)-inducible cellular responses and stress shock proteome in *Stenotrophomonas* sp. OK-5. *Curr. Microbiol.* **49**, 346–352.

Jackson RG, Rylott EL, Fournier D, Hawari J, and Bruce NC. 2007. Exploring the biochemical properties and remediation applications of the unusual explosive-degrading P450 system XplA/B. *Proc. Nat. Acad. Sci. USA* **104**, 16822–16827.

Juhasz AL and Naidu R. 2007. Explosives: fate, dynamics, and ecological impact in terrestrial and marine environments. *Rev. Environ. Contam. Toxicol*. **191**, 163–215.

Kim SI, Kim SJ, Nam MH, Kim S, Ha KS, Oh KH, Yoo JS, and Park YM. 2002. Proteome analysis of aniline-induced proteins in *Acinetobacter lwoffii* K24. *Curr. Microbiol.* **44**, 61–66.

Kitts CL, Cunningham DP, and Unkefer PJ. 1994. Isolation of three hexahydro-1,3,5-trinitro-1,3,5-triazine-degrading species of the family *Enterobacteriaceae* from nitramine explosive-contaminated soil. *Appl. Environ. Microbiol*. **60**, 4608–4711.

Lee BU, Choi MS, and Oh KH. 2013. Comparative analysis of explosive RDX-induced proteomes in the *Pseudomonas* sp. HK-6 wild-type strain and its *rpoH* mutant strain. *Biotechnol. Bioprocess Eng.* **18**, 1224–1229.

Lee BU, Choi MS, and Oh KH. 2015. Characterization and proteomic analysis of the *Pseudomonas* sp. HK-6 *xenB* knockout mutant under RDX (hexahydro-1,3,5-trinitro-1,3,5-triazine) stress. *Curr. Microbiol.* **70**, 119–127.

Lee BU, Park SC, Cho YS, Kahng HY, and Oh KH. 2008a. Expression and characterization of the TNT nitroreductase of *Pseudomonas* sp. HK-6 in *Escherichia coli*. *Curr. Microbiol.* **56**, 386–390.

Lee BU, Park SC, Cho YS, and Oh KH. 2008b. Exopolymer biosynthesis and proteomic changes of *Pseudomonas* sp. HK-6 under stress of TNT (2,4,6-trinitrotoluene). *Curr. Microbiol.* **57**, 477–483.

Lee DC, Stenland CJ, Hartwell RC, Ford EK, Cai K, Miller LC, Gilligan KJ, Rubenstein R, Fournel M, and Petteway Jr SR. 2000. Monitoring plasma processing steps with a sensitive western blot assay for the detection of the porin protein. *J. Virol. Methods* **84**, 77–89.

Lorenz A, Rylott EL, Strand SE, and Bruce NC. 2012. Towards engineering degradation of the explosive pollutant hexahydro-1,3,5-trinitro-1,3,5-triazine in the rhizosphere. *FEMS Microbiol. Lett.* **340**, 49–54.

McCormick NG, Cornell JH, and Kaplan AM. 1981. Biodegradation of hexahydro-1,3,5-trinitro-1,3,5-triazine. *Appl. Environ. Microbiol*. **42**, 817–823.

McLellan W, Hartley WR, and Brower M. 1992. Hexahydro-1,3,5-trinitro-1,3,5-triazine (RDX), pp. 132–180. *In* Roberts WC and Hartley WR. (eds.), Drinking water health advisory: Munition, Lewis Publishers, Boca Raton, USA.

Miller JH. 1972. Experiments in molecular genetics, Cold Spring Harbor Laboratory, New York, NY, USA.

Ng LK, Sherburne R, Taylor DE, and Stiles ME. 1985. Morphological forms and viability of *Campylobacter* species studied by electron microscopy. *J. Bacteriol.* **164**, 338–343.

Nizam S, Gazara RK, Verma S, Singh K, and Verma PK. 2014. Comparative structural modeling of sox Old Yellow Enzymes (OYEs) from the necrotrophic fungus *Ascochytarabiei*: insight into novel OYE classes with differences in cofactor binding, organization of active site residues and stereopreferences. *PLoS One* **9**, e95989.

Orville AM, Manning L, Blehert DS, Fox BG, and Chambliss GH. 2004. Crystallization and preliminary analysis of xenobiotics reductase B from *Pseudomonas fluorescence* I-C. *Acta Crystallogr.*

D Biol. Crystallogr. **60**, 1289–1291.

Osman JL and Klausmeier RE. 1973. Microbial degradation of explosives. *Dev. Ind. Microbiol.* **14**, 247–252.

Pak JW, Knoke KL, Noguera DR, Fox BG, and Chambliss GH. 2000. Transformation of 2,4,6-trinitrotoluene by purified xenobiotic reductase B from *Pseudomonas fluorescens* I-C. *Appl. Environ. Microbiol.* **66**, 4742–4750.

Perkins DN, Pappin DJ, Creasy DM, and Cottrell JS. 1999. Probability-based protein identification by searching sequence databases using mass spectrometry data. *Electrophoresis* **20**, 3551–3567.

Ramos JL, Duque E, Huertas MK, and Haidour A. 1995. Isolation and expression of catabolic potential of a *Pseudomonas putida* strain able to grow in presence of high concentrations of aromatic hydrocarbons. *J. Bacteriol.* **177**, 3911–3916.

Ronen Z, Yanovich Y, Goldin R, and Adar E. 2008. Metabolism of the explosive hexahydro-1,3,5-trinitro-1,3,5-triazine (RDX) in a contaminated valdose zone. *Chemosphere* **73**, 1492–1498.

Sikkema J, de Bont JAM, and Poolman B. 1995. Mechanisms of membrane toxicity of hydrocarbons. *Microbiol. Rev.* **59**, 201–222.

Spiegelhauer O, Werther T, Mende S, Knauer SH, and Dobbek H. 2010. Determinants of substrate binding and protonation in the flavoenzyme xenobiotic reductase A. *J. Mol. Biol.* **403**, 286–298.

Williams RE and Bruce NC. 2002. 'New uses for an old enzyme'-the old yellow enzyme of flavoenzymes. *Microbiology* **148**, 1607–1614.